CONF-820738--6

SHELL STRUCTURE AT HIGH SPIN AND THE INFLUENCE ON NUCLEAR SHAPES

CONF-820738--6
DE83 008504

T. L. Khoo, P. Chowdhury, I. Ahmad, J. Borggreen,[a] H. Emling,[b] D. Frekers, R. V. F. Janssens
Argonne National Laboratory, Argonne, Illinois 60439, USA

A. Pakkanen,[c], Y. H. Chung, P. J. Daly, S. R. Faber, Z. Grabowski, H. Helppi,[c] M. Kortelahti and J. Wilson
Purdue University, W. Lafayette, Indiana 47907, USA

Abstract

Nuclear structure at high spin is influenced by a combination of liquid-drop and shell-structure effects. For $N < 86$ both contribute towards the occurrence along the yrast line of high-spin oblate aligned-particle configurations. Shell effects are mainly responsible for the prolate deformation of nuclei with $N > 90$. The competition between oblate and prolate driving effects leads to a prolate-to-oblate shape transition in $^{154}_{66}Dy_{88}$. The role of rotation-aligned configurations in the shape change is discussed.

In the Strutinsky formalism the energy is given[1] as

$$E = \left(\sum_i e_i - \sum_i \tilde{e}_i\right) + E_{LD}, \qquad (1)$$

where e_i is the single-particle energy, $\tilde{e}_i$ the Strutinsky-smeared single-particle energy and E_{LD} the liquid drop energy. The term in brackets gives the shell-energy correction to the liquid-drop term. For a rotating system the latter is

$$E_{LD} \sim \frac{\hbar^2}{2\mathcal{J}_{LD}} I(I+1) \qquad (2)$$

where $\mathcal{J}_{LD}$ is the moment of inertia given by the liquid-drop model.[2] Before the onset of fission, the largest and smallest values of $\mathcal{J}_{LD}$ are obtained for rotation about the symmetry axis for oblate and prolate shapes, respectively. For high-spin states a large negative shell energy is obtained either when a

gap in the single-particle spacing develops or when the Fermi level is located in a cluster of high-j orbits.

An example of the importance of the shell-correction term is given by the Hf nuclei with A ~ 176. Figure 1 shows that for I > 16 the yrast states of ^{176}Hf are formed from high-K band heads (Ref. 3), corresponding to rotation about the prolate symmetry axis, although the liquid drop term in Eq. (1) would have the largest value for this mode. The high-K states form part of the yrast line in this mass region because both the proton and neutron Fermi levels are embedded among clusters of high-Ω orbitals, leading to a large shell energy.

In this talk we shall discuss the influence of shell structure on nuclear shapes at high spin and, in particular, on the change in shape across the N = 88 transitional region. We

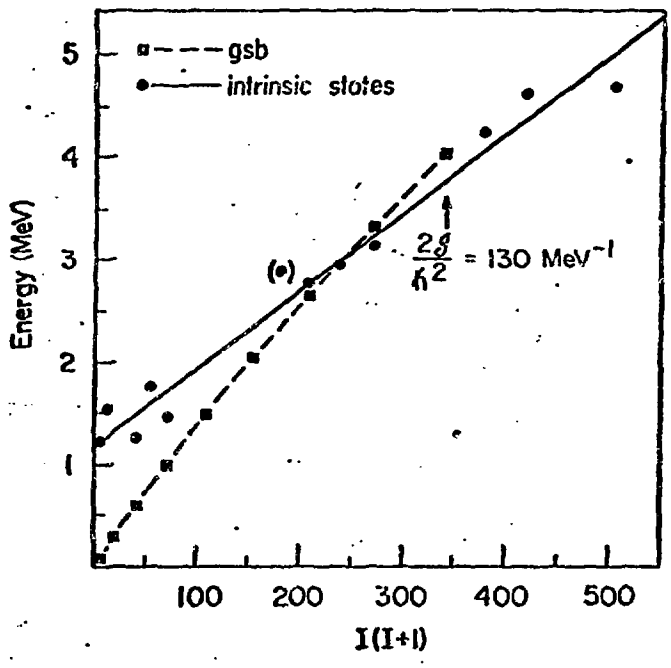

Fig. 1. Plot for ^{176}Hf of lowest band-head energies (circles) and ground-band energies (squares) vs I(I + 1). Note that for I > 16 the high-K band heads are lower in energy than the ground-band members of the same spin.

shall consider nuclear structure as a function of both spin I and neutron number N within one common framework. The Hamiltonian for a rotating system is given[4] by

$$\hat{H} = \hat{H}_o - \epsilon\hat{Q}_o - \Delta(\hat{P} + \hat{P}^\dagger) - \omega\hat{I}_x - \lambda\hat{N} \qquad (3)$$

where the Lagrange multipliers, ω and λ, have been introduced to constrain the spin and the particle numbers: $I_x = \langle\hat{I}_x\rangle$ and $N = \langle\hat{N}\rangle$. ω is the rotational frequency and λ is the Fermi energy. From Eq. (3) it is seen that spin and particle number can be treated on an equal footing.

Figure 2 summarizes our recent knowledge about nuclear shapes as a function of both neutron number N and spin I, using a plot first introduced in Ref. 4. For I = 0 it is well known that nuclei are spherical (or nearly so) for N < 88, whereas a sudden onset of prolate shape occurs at N = 90. At high spins nuclei with N < 86 begin to acquire oblate shapes ($\epsilon \sim 0.1 - 0.2$) as an increasing number of particles align along a symmetry axis (Ref. 5-7). The nuclei with N > 90 retain their prolate shapes at high spin.

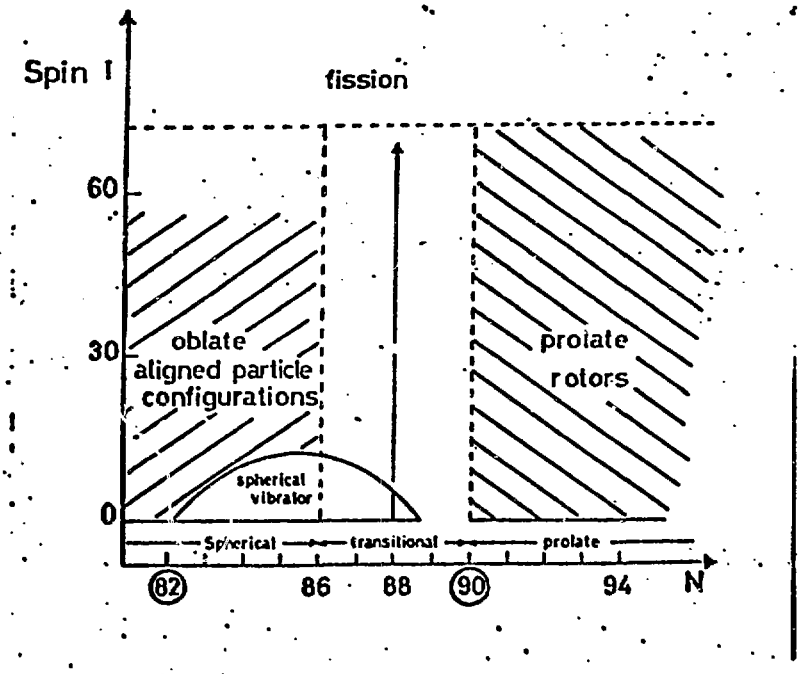

Fig. 2. Summary of recent knowledge of nuclear shapes as a function of neutron number N and spin I.

The different modes for generating angular momentum as a function of I and N are shown in Fig. 3. For N < 86 individual nucleons align their spins along a symmetry axis. The large spatial concentration of the orbits around the equator and the concomitant core polarization lead to an oblate deformation along the yrast line with $\beta \sim 0.1 - 0.2$ (Refs. 5-7).

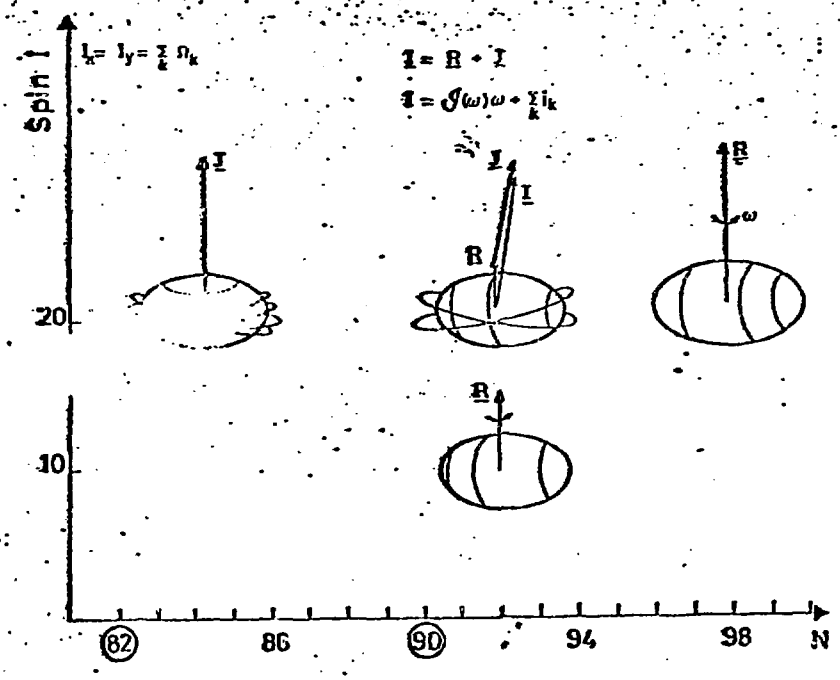

Fig. 3. Different modes of generating angular momentum as a function of neutron number N and spin I.

The oblate aligned-particle configurations become yrast because of contributions from both liquid drop and shell-energy terms in Eq. 1. E_{LD} in Eq. (1) and (2) is a minimum for rotation of an oblate liquid drop about its symmetry axis. In addition, the shell energy is large because of a concentration of high-j orbits ($\pi h_{11/2}$, $\nu f_{7/2}$, $\nu h_{9/2}$, $\nu i_{13/2}$) around the Fermi levels. Furthermore, the high-Ω substates of these orbits have large mass quadrupole moments and large energy gains with increasing oblate deformation. Without the shell-energy contribution the oblate configurations would probably not be yrast at high spin. A measure of this contribution is given by the slope of the yrast line in ^{147}Gd. A I=49/2 isomer has $\beta \sim 0.2$ (Ref. 8), and the states of higher spins have a similar deformation according to the calculations of Døssing et al.[7] For $I > 49/2$, this would lead to an effective moment of inertia, $2\mathcal{J}_{eff}/\hbar^2 \sim 2\mathcal{J}_o/\hbar^2 (1 + 0.6\,\beta)$, of 127 MeV^{-1}. (The rigid sphere value is $2\mathcal{J}_o/\hbar^2 = 113$ MeV^{-1}). However, the slope of the experimental yrast line[6,10] on an E vs I(I + 1) plot gives $2\mathcal{J}_{eff}/\hbar^2 = 142$ MeV^{-1}, reflecting an additional contribution from shell structure.

For $N > 90$ the yrast spins usually arise from collective rotation of prolate shapes about an axis perpendicular to the symmetry axis. Near $N = 90$ rotation alignment[9] occurs for $I \gtrsim 16$ and the total angular momentum is the sum of contributions from collective rotation and from the aligned spins of high-j particles (usually $\nu i_{13/2}$ and $\pi h_{11/2}$).

It is well known that prolate deformation occurs because of shell-structure effects. An interesting discussion on this point has recently been given by Bengtsson et al.[4] Figure 4, which is reproduced from Ref. 4, shows calculated curves of N vs λ for spherical and deformed shapes. The slope on such a plot reflects the level density around the Fermi surface and thus is inversely related to the shell energy. With increasing N the slope in the spherical case becomes larger than that for the deformed case. Consequently, the magnitude of the shell energy for the former becomes smaller than that for the latter. Thus a switch from spherical to deformed shape occurs. Figure 5, also reproduced from Ref. 4, shows plots of N vs λ for different spin values of even-A Dy isotopes. These plots, referred to as backbending

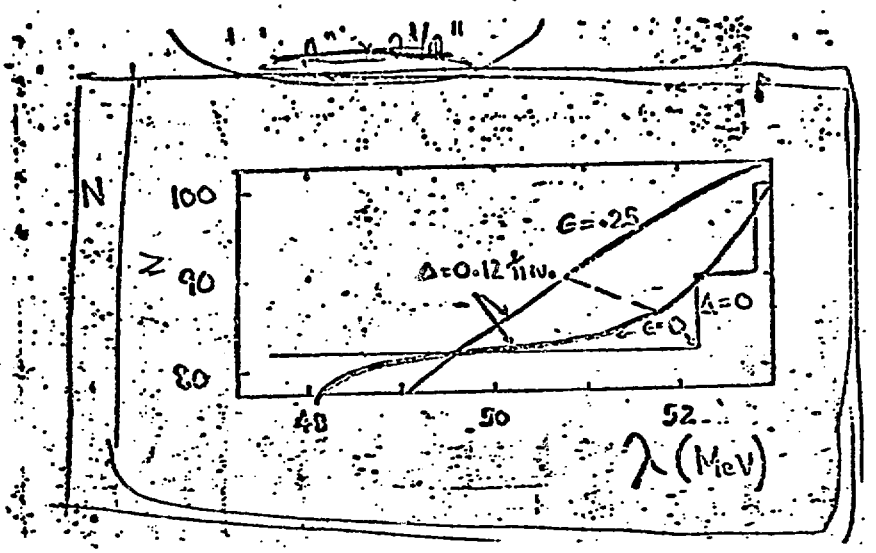

Fig. 4. Calculated plots, from Ref. 4, of neutron number N vs Fermi energy λ for spherical shape, $\varepsilon = 0 (\Delta = 0$ and $\Delta = 0.12\ \hbar\omega_0)$ and for deformed shape, $\varepsilon = 0.25$ ($\Delta \doteq 0.12\ \hbar\omega_0$). When the energy for the deformed shape becomes less than that for the spherical shape, a transition between the $\varepsilon = 0$ and $\varepsilon = 0.25$ curves occurs, giving rise to 'backbending in gauge space' (Ref. 4).

plots in gauge-space[4], show that the transition from spherical to deformed shapes occurs around N = 90 for the I = 0 ground state. However, with increasing spin the transition occurs at lower neutron number. Thus ^{154}Dy, with N = 88, is transitional in the ground state, but is decidedly prolate at higher spins.

Prolate deformation arises from the participation of many orbits which are coupled by the deformed field. (This is reflected in the convex curvature of low-Ω orbits in a Nilsson diagram.) On the other hand, oblate deformation for N < 86 has its origins in the alignment of a few (4-10) nucleon orbits. Thus, the oblate deformation may be rather delicate and may not be stable with respect to increasing temperature (i.e. excitation energy above the yrast line) or rotation about an axis perpendicular to the symmetry axis. (See also the discussion in Ref. 11).

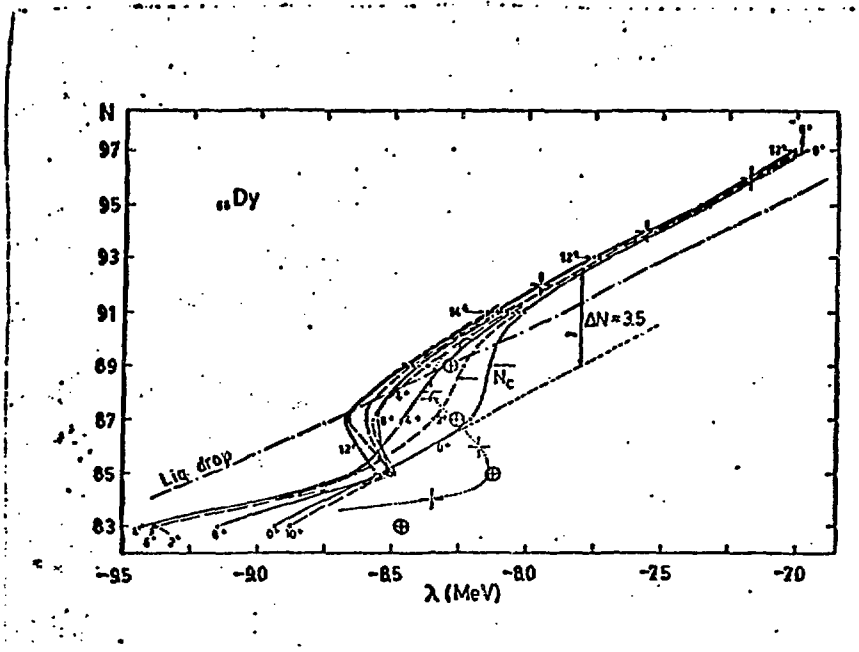

Fig. 5. N vs λ for various spin states of even Dy-isotopes (reproduced from Ref. 4.) The values of $\lambda = \frac{\partial E}{\partial N} \sim \frac{E(Z,N+1,I)-E(Z,N-1,I)}{2}$ have been calculated from experimental masses and yrast spectra.

Since oblate-driving effects are prevalent for N < 86 and prolate shell-effects dominate for N > 90, a competition between the two effects should occur in the transitional region. Thus it is of particular interest to establish the high-spin structure of the N = 87 and 88 nuclei. There is the possibility of observing for the first time a prolate-to-oblate shape change at high spin. Furthermore, the data will fill the knowledge gap in Fig. 1, leading to a comprehensive understanding of shape transition as a function of both neutron number and spin.

The Argonne-Purdue collaboration is currently investigating the high-spin structure of ^{153,154}Dy and the results on ^{154}Dy are reported here. The (^{34}S,4n) reaction has been utilized, with 145-165 MeV beams from the Argonne superconducting linac. An extensive set of γ-spectroscopy experiments were performed, including measurements of γ-γ coincidences, angular distributions, excitation functions and lifetimes. In all experiments a large NaI detector was used, either as a sum spectrometer or multiplicity filter, to enhance the reaction channel of interest. The level scheme for ^{154}Dy is shown in Fig. 6 (Ref. 12). For the positive-parity levels a plot of $2\mathcal{J}/\hbar^2$ vs $(\hbar\omega)^2$ shows two backbends at I = 16 and 30 (Fig. 7).

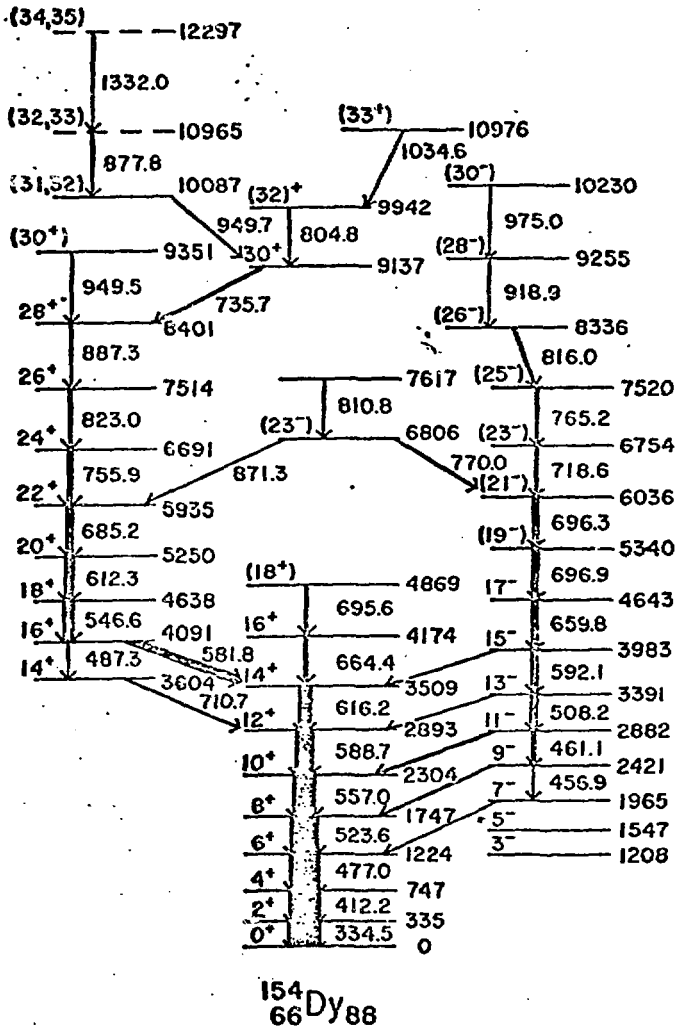

$^{154}_{66}Dy_{88}$

Fig. 6. Level scheme of ^{154}Dy.

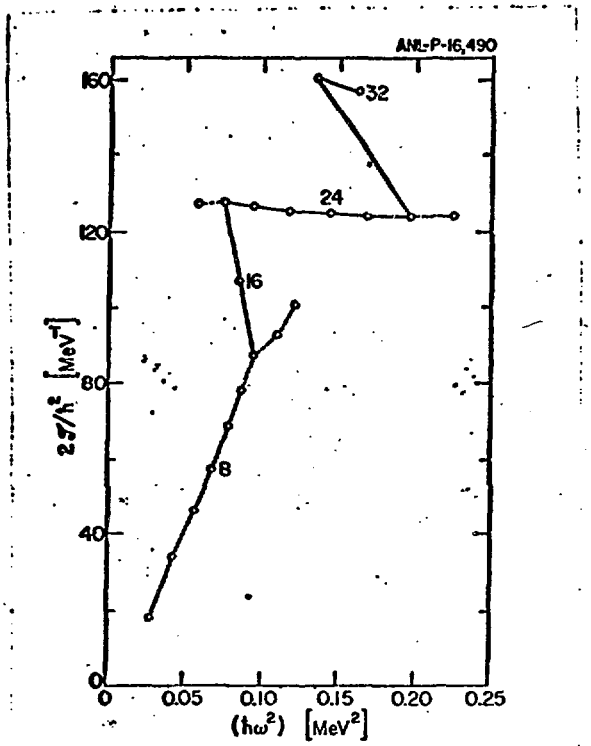

Fig. 7. Plot of $2\mathcal{I}/\hbar^2$ vs $(\hbar\omega)^2$ for even parity states in ^{154}Dy.

No nanosecond isomers were observed in ^{154}Dy in electronic timing measurements. Thus recoil-distance lifetime measurements were performed with a plunger constructed by D. C. Radford (Yale University) and another one recently constructed at Argonne. The latter fits inside the NaI sum spectrometer, with the motion of the stopper determined by three microprocessor-controlled DC-motor actuators.

From the measured lifetimes we have derived, for the positive parity yrast levels, the quantity $Q_0(\text{eff}) = [B(E2\ I \to I-2)\ 16\pi/5]^{1/2}/\langle I\ 2\ 0\ 0 | I{-}2\ 0\rangle$. This gives the usual intrinsic quadrupole moment Q_0 for a K = 0 band of an axially symmetric rotor, and for I >> K in general, without the constraint of axial symmetry. As seen in Fig. 8, Q_0(eff) increases between spins 2 and 6, stays high up to spin 20, and then gradually decreases. In terms of single-particle or Weisskopf units (w.u.), the E2 rates increase from 99 w.u. to a maximum of ~286 w.u. and then decrease to ~35 w.u. between I = 26 and 32. The highest energy states at 10.976 and 12.297 MeV have combined state and feeding times of 6 ± 1 and 5 ± 1 ps, respectively. (We have recently performed another measurement which should yield results of higher precision than those shown in Fig. 8.)

Up to spin 32, the positive parity yrast levels are characteristic of a collective rotor with intermediate deformation. The yrast transition energies increase monotonically, except near the backbends (see Figs. 6 and 7), while the levels are connected by only stretched E2 transitions

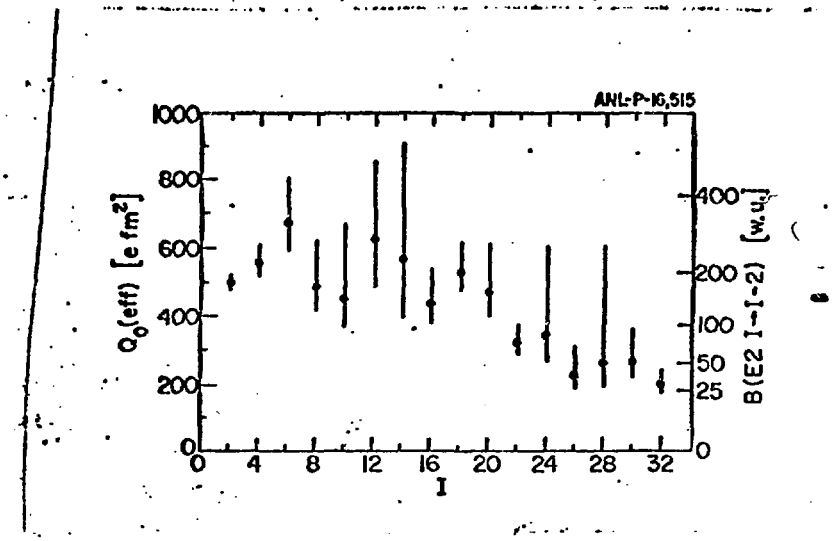

Fig. 8. Spin dependence of Q_0(eff) defined as $[B(E2\ I \to I-2)16\pi/5]^{1/2}/\langle I\ 2\ 0\ 0 | I-2\ 0\rangle$.
For I > 10 the Clebsch-Gordon coefficient is almost constant and the right-hand ordinate shows the approximate B(E2) in Weisskopf units.

which are enhanced (Fig. 8). A prolate shape at intermediate spin is suggested by the systematic trends[4] in this mass region and by the first backbend, which is due to the rotational alignment[9] of a neutron in the beginning of the $i_{13/2}$ shell.

However, above spin 32 a change to few-particle structure occurs. The transition energies cease to increase smoothly. Predominantly dipole transitions (878 and 1035 keV) appear, terminating the hitherto uninterrupted cascade of stretched E2 gamma rays. In addition, the positive parity sequence begins to fragment above spin 28, a behavior quite different from that of the typical backbending nucleus, where usually only a single yrast branch is observed at the highest spins. Finally, the combined state and feeding times of the highest observed levels with I = (33^+) and I = 34 or 35 (6 and 5 ps, respectively) are significantly slower than the typical value of $\lesssim$ 0.5 ps observed at high spin in collective rotors like ^{156,158}Dy (Ref. 13), but are similar to those observed[6] in ^{152}Dy, which exhibits aligned-particle nature. It is likely that aligned-particle configurations similar to those in neighboring ^{152}Dy are involved, since only these would lie at sufficiently low energy. As in ^{152}Dy, these configurations would lead to an

oblate mass distribution. Thus, it appears that the yrast states of ^{154}Dy are oblate above spin 32.

The spin dependence of Q_0(eff) shown in Fig. 8 already reflects a decrease in collectivity between I = 20 and 32. For a rigidly rotating triaxial body Q_0(eff) is related to the parameters β and γ, characterizing quadrupole deformation and axial asymmetry, by the expression[14]

$$Q_0(\text{eff}) \propto \beta \cos(30^0 - \gamma).$$

Since the shape is most likely prolate (γ = 0°) for I < 20 and oblate (γ = -60°) for I > 32, the decrease in Q_0(eff) probably has a substantial contribution from a change in γ [Fig. 9(a)]. [The measurement of only Q_0(eff) does not allow for the extraction of β and γ separately. However, if the decrease in Q_0(eff) were due to a variation of γ only, values of γ around -35° would be obtained between spins 26 and 32.]

A reduction in collectivity at high spin ($I \gtrsim 16$) has also been observed in ^{156}Dy and ^{158}Dy by Emling et al.,[13] who have similarly attributed it to the onset of triaxiality. In comparing the even Dy isotopes with A = 154-158 the trend is that the reduction is more pronounced for the lighter isotopes; furthermore, only in ^{154}Dy has the limit of single-particle transition rates been observed. These observations are consistent with the fact that prolate shell effects become more firmly established as N increases beyond 90.

The decrease in collectivity in ^{154,156,158}Dy happens after the first backbend in all three cases. In addition, the transition to aligned-particle structure occurs shortly after the second backbend in ^{154}Dy. Thus, it seems that rotation alignment, which causes backbending, plays an important role in shape transition. Indeed, when the Coriolis force aligns the high-j $vi_{13/2}$ orbit along the rotation vector, the orbit acquires an oblate mass distribution with respect to this vector. This is illustrated in Fig. 10. The aligned particles will polarize the core, inducing a departure from axial symmetry. The degree of asymmetry will depend on the polarizability, which would tend to be large in a transitional nucleus such as ^{154}Dy. After the second backbend--which is probably due to the additional

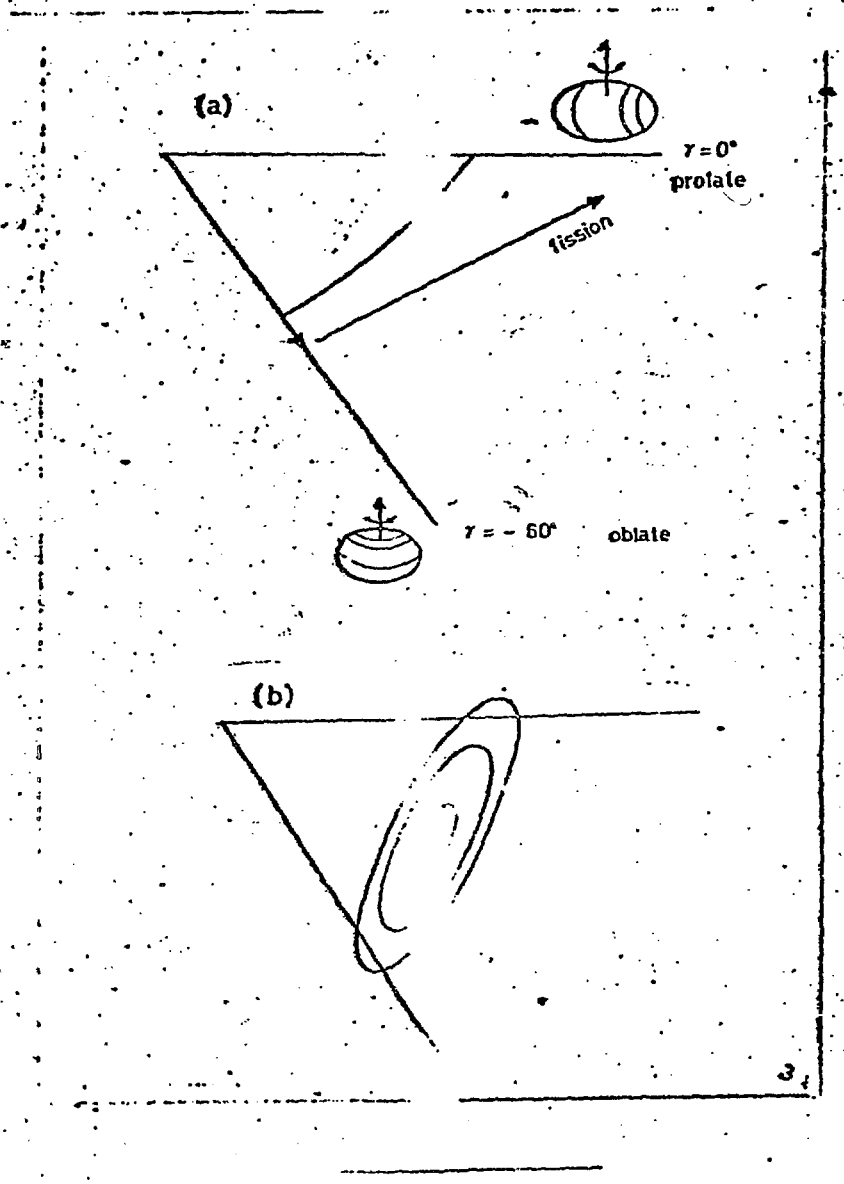

Fig. 9. (a) Schematic representation of the transition from prolate to triaxial to oblate shapes, which probably occurs in ^{154}Dy. (b) Schematic illustration of the potential energy surface, calculated in Ref. 15, which is flat in the γ direction.

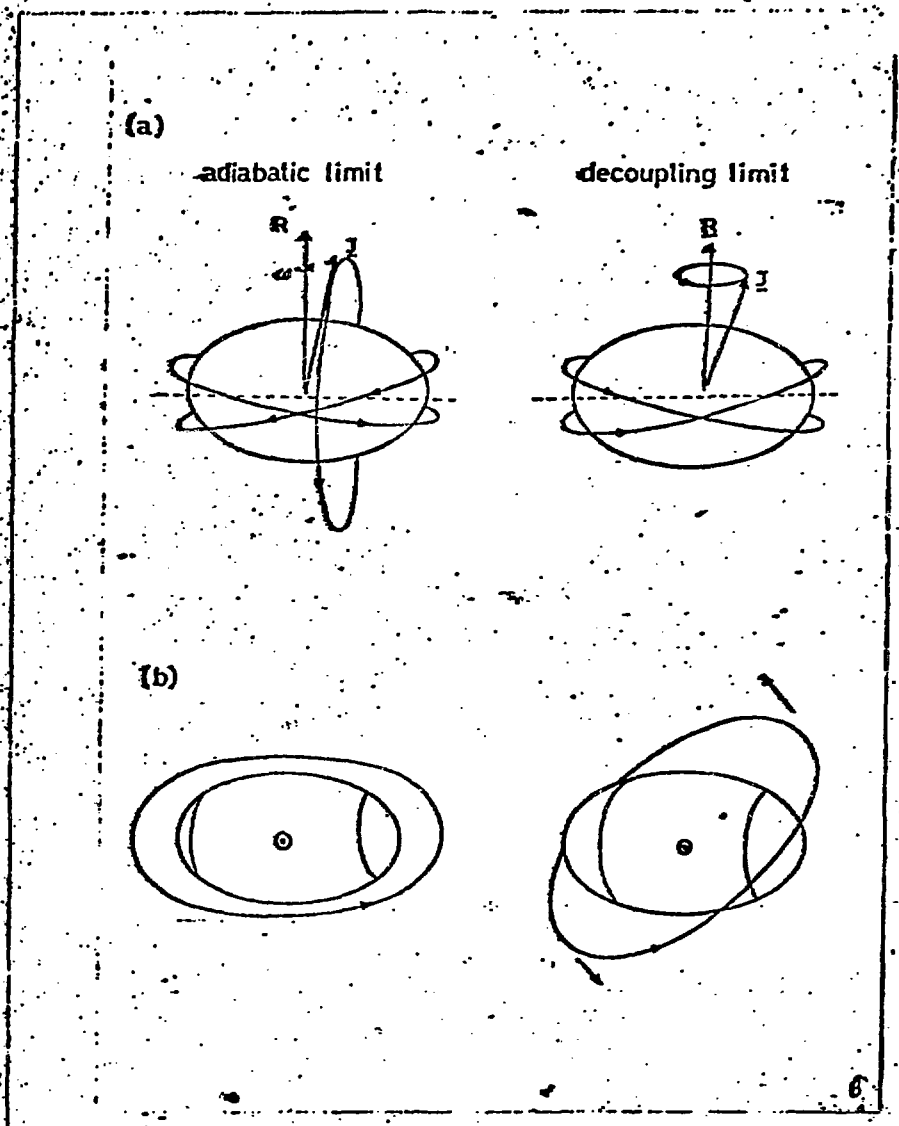

Fig. 10. (a) Precession of the particle-spin vector about the symmetric and perpendicular axes in the adiabatic (strong-coupling) and rotation-aligned (decoupling) limits. (b) Particle orbit, viewed along the perpendicular axis in the rotating frame for the two limits indicated. In the decoupling limit, the precession of the particle orbit around the perpendicular axis leads to an oblate mass distribution with respect to this axis for the orbit.

alignment of a $\pi h_{11/2}$ pair--the polarization will increase, particularly with the alignment of both neutrons and protons. Thus a transition to oblate shapes could occur, as in the lighter Dy isotopes, especially with the prolate-driving shell effects not yet firmly established at N = 88.

The transition from prolate to oblate shapes via rotation-aligned structures represents a process whereby aligned particles contribute a step-wise increase in angular momentum. For the prolate ground band the angular momentum consists entirely of only a collective component which is perpendicular to the symmetry axis. In the rotation-aligned bands the angular momentum is generated by both aligned-particle and collective spins along the perpendicular axis. In the oblate limit this axis becomes the symmetry axis along which only particle spins align. These points are illustrated in Fig. 11 (b) and (c), where the rotation frequency of the core and the spin from particle alignment are plotted as a function of time following compound nucleus formation. It is interesting to compare the fluctuations in the frequency of the nuclear core with the fluctuations in the rotational frequency of the surface of a rotating neutron star [see Fig. 11(a)]. The star quakes in the latter correspond to $\frac{\Delta\Omega}{\Omega} \sim 10^{-6}$, while the 'nuclear quakes' with $\frac{\Delta\omega}{\omega} \sim 0.2$ are relatively much more violent!

One reason for the transition to oblate shapes is the smaller energy increment per unit spin associated with these shapes. This can be seen in Fig. 12, which shows plots of E vs I(I + 1) for ^{152,154,156}Dy. The average slope for oblate aligned-particle configurations in ^{152}Dy (1/147 MeV) is smaller than that for the rotation-aligned $i_{13/2}$ band in ^{154}Dy (1/124 MeV). For ^{156}Dy, although the slope of the prolate yrast line is steeper than that of the oblate one in ^{152}Dy, the yrast states of the former generally lie lower in energy. A transition to oblate shapes in ^{156}Dy is thus not expected until at least I ~ 40. This is also consistent with the fact that the prolate-driving effects are more firmly entrenched in ^{156}Dy than in ^{154}Dy. As a corollary, one expects that the collective excitations in ^{153}Dy

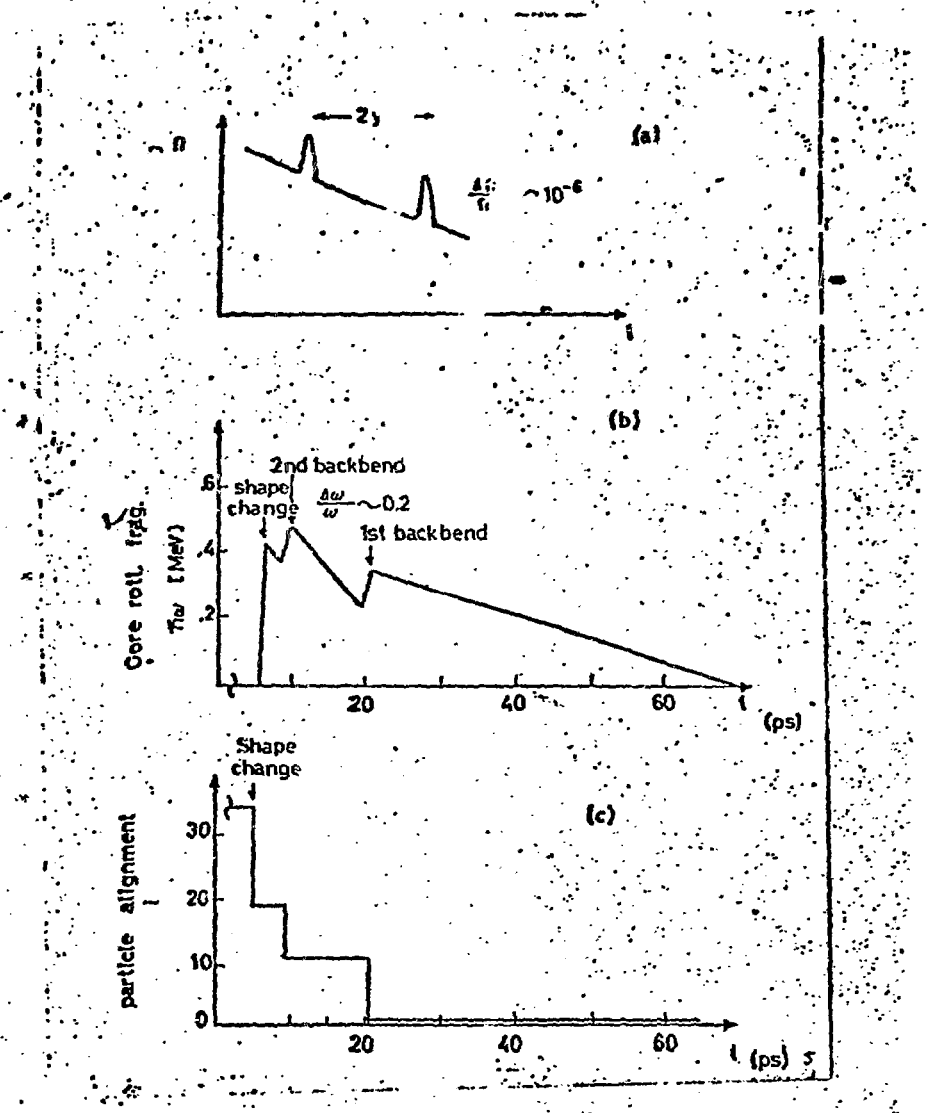

Fig. 11. (a) Rotational frequency fluctuation of the surface of a neutron star (pulsar). (b) Rotational frequency of the nuclear core as a function of time after compound nucleus formation. The values for $\hbar\omega$ and t are approximately those for ^{154}Dy following the (^{34}S,4n) reaction at 160 MeV. Abrupt changes in frequency correspond either to the departure from oblate shapes or to backbends. (c) Aligned particle spin i as a function of t [defined in (b)]. Changes in i give rise to corresponding fluctuations in the core rotational frequency.

will give way to aligned-particle configurations at rather low spins. Preliminary analyses of our data for ^{153}Dy indicate an isomer with spin around 49/2, consistent with this expectation.

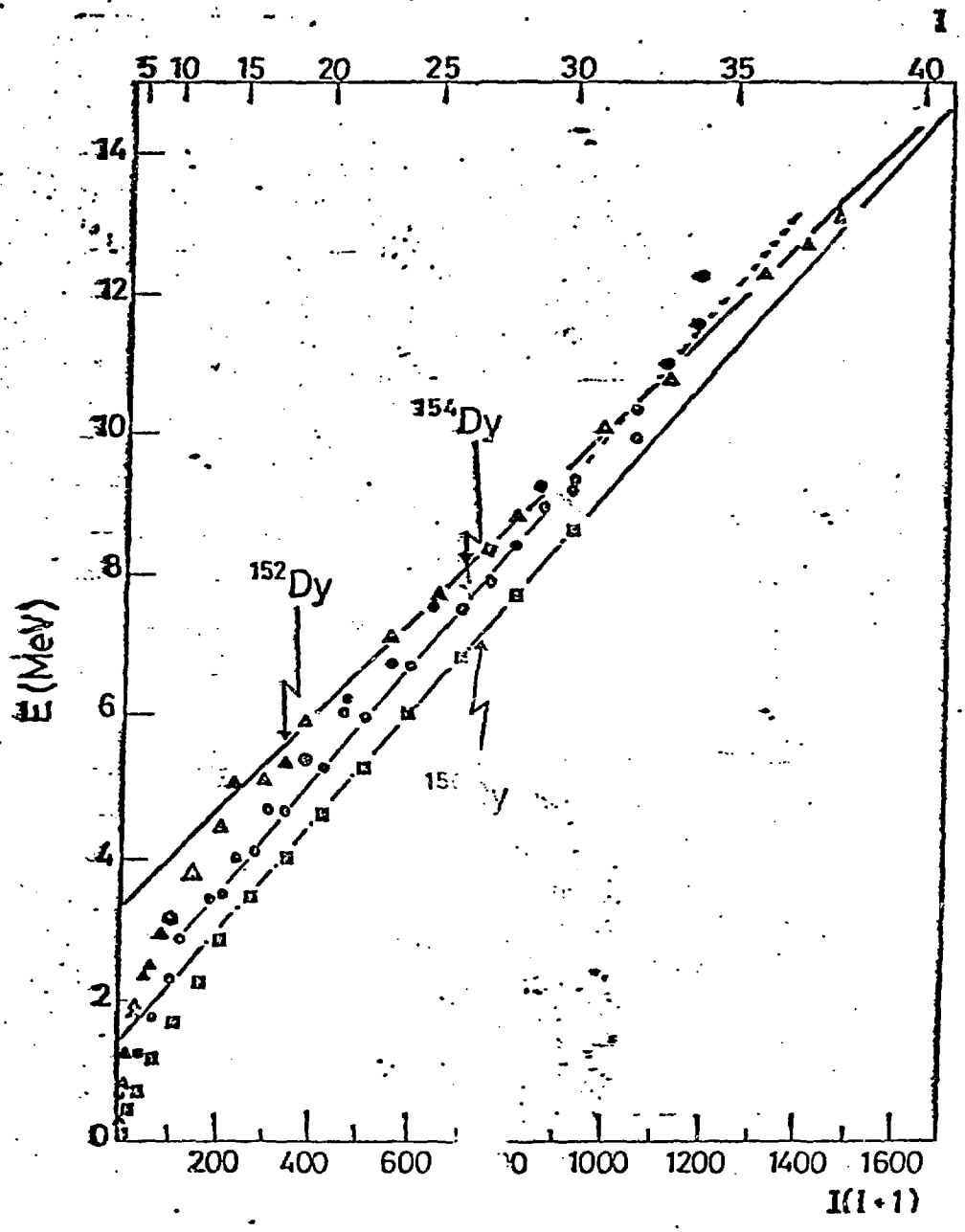

Fig. 12. Plots of E vs I(I + 1) for ^{152}Dy (▲), ^{154}Dy (○) and ^{156}Dy (■). The inverse of the average slopes for the 3 cases yield $2\mathcal{J}_{eff}/\hbar^2$ = 147, 124 and 127 MeV^{-1}, respectively.

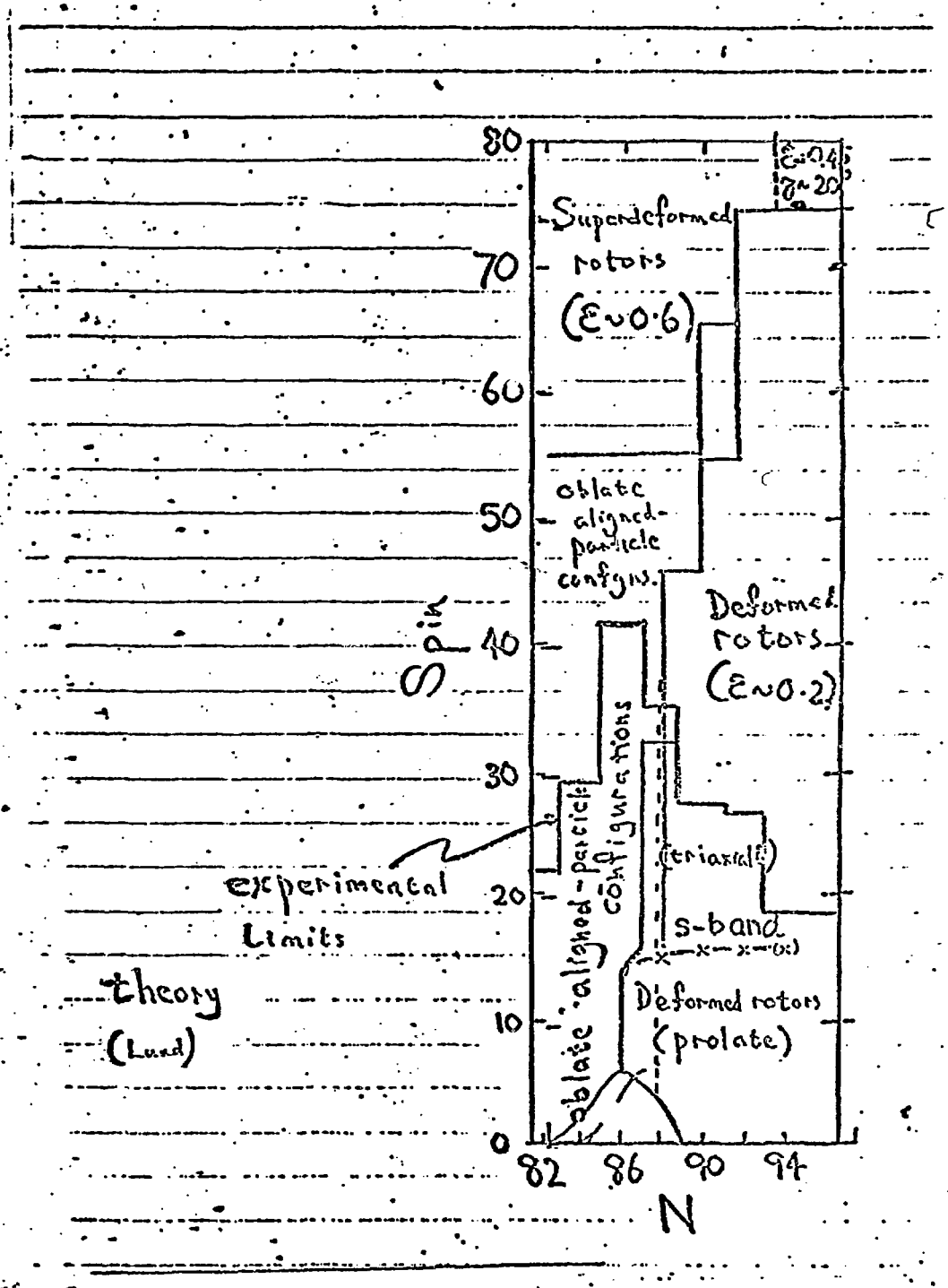

Fig. 13. Current knowledge about the different 'phases' of even Dy nuclei as a function of spin and neutron number. Also shown are the 'phases' predicted in Ref. 4 and 15.

The present information on even-A Dy isotopes is summarized on an I vs N plot (Fig. 13), in the manner suggested by Bengtsson et al.[4]. The different 'phases' nuclei undergo as a function of increasing spin and neutron number may be observed on such a diagram.

Figure 13 also indicates the theoretical predictions of Andersson et al.[15]. It is seen that a transition from prolate to oblate in ^{154}Dy is predicted, but at a higher spin ($I \sim 45$) than experimentally observed ($I = 33$). The calculations of Ref. 15 show rather flat potential energy surfaces in the γ direction [as schematically illustrated in Fig. 9(b)] leading to some difficulty in accurately predicting the transition spin. In any event, pairing which is known to have a profound effect on rotation alignment, has not been included. It would be important to perform further calculations with pairing included in order to gain a firmer understanding of the microscopic basis for the shape transition.

References and Footnotes

[a]Permanent address: Niels Bohr Institute, Risø, Denmark.

[b]Permanent address: GSI, Darmstadt, W. Germany.

[c]Permanent address: University of Jyväskylä, Jyväskylä.

1. See e.g., K. Neergaard, Proc. Nuclear Physics Workshop, Trieste, 5-30 October 1981, ed. R. A. Broglia et al. (North-Holland).
2. S. Cohen, F. Plasil and W. J. Swiatecki, Ann. Phys. 82, 557 (1974).
3. T. L. Khoo, F. M. Bernthal, R. G. H. Robertson and R. A. Warner, Phys. Rev. Lett. 37, 823, (1976).
4. R. Bengtsson, Jing-ye Zhang and S. Åberg, Phys. Lett. 105B, 5 (1981).
5. T. L. Khoo, J. Phys. (Paris) Colloq. C10, 9 (1980).
6. B. Haas, D. Ward, H. R. Andrews, O. Häusser, A. J. Ferguson, J. F. Sharpey-Schafer, T. K. Alexander, W. Trautmann, D. Horn, P. Taras, P. Skensved, T. L. Khoo, R. K. Smither, I. Ahmad, C. N. Davids, W. Kutschera, S. Levenson and C. L. Dors, Nucl. Phys. A362, 254 (1981).
7. T. Døssing, K. Neergaard and H. Sagawa, Phys. Scr. 24, 258 (1981).

8. O. Häusser, H. E. Mahnke, J. F. Sharpey-Schafer, M. L. Swanson, P. Taras, D. Ward, H. R. Andrews and T. K. Alexander, Phys. Rev. Lett. 44, 132, (1980).

9. F. S. Stephens, Rev. Mod. Phys. 47, 43 (1975).

10. O. Bakander, C. Baktash, J. Borggreen, J. B. Jansen, J. Kownacki, J. Pederson, G. Sletten, D. Ward, H. R. Andrews, O. Häusser, P. Skensved and P. Taras, to be published in Nucl. Phys. A.

11. T. L. Khoo, J. Borggreen, P. Chowdhury, I. Ahmad, R. K. Smither, S. R. Faber, P. J. Daly, C. L. Dors, and J. Wilson, Phys. Scr. 24, 283 (1981).

12. A. Pakkanen, Y. H. Chung, P. J. Daly, S. R. Faber, H. Helppi, J. Wilson, P. Chowdhury, T. L. Khoo, I. Ahmad, J. Borggreen, Z. W. Grabowski, and D. C. Radford, Phys. Rev. Lett. 48, 1530 (1982).

13. H. Emling, E. Grosse, D. Schwalm, R. S. Simon and H. J. Wollersheim, Phys. Lett. 98B, 169 (1981), H. Emling, GSI Preprint No. 81-40 (to be published).

14. J. Liotta and R. A. Sorensen, Nucl. Phys. A297, 136 (1978).

15. C. G. Andersson, R. Bengtsson, T. Bengtsson, J. Krumlinde, G. Leander, K. Neergaard, P. Olander, J. A. Pinston, I. Ragnarsson, Z. Szymanski and S. Åberg, Phys. Scr. 24, 266 (1981).

DISCLAIMER